

LA-UR-18-28264

Approved for public release; distribution is unlimited.

Title: Beam Dynamics for Scorpis with the CDR end-to-end tune: II.
Short-pulse stability

Author(s): Ekdahl, Carl August Jr.

Intended for: Report

Issued: 2018-08-29

Disclaimer:

Los Alamos National Laboratory, an affirmative action/equal opportunity employer, is operated by the Los Alamos National Security, LLC for the National Nuclear Security Administration of the U.S. Department of Energy under contract DE-AC52-06NA25396. By approving this article, the publisher recognizes that the U.S. Government retains nonexclusive, royalty-free license to publish or reproduce the published form of this contribution, or to allow others to do so, for U.S. Government purposes. Los Alamos National Laboratory requests that the publisher identify this article as work performed under the auspices of the U.S. Department of Energy. Los Alamos National Laboratory strongly supports academic freedom and a researcher's right to publish; as an institution, however, the Laboratory does not endorse the viewpoint of a publication or guarantee its technical correctness.

Beam Dynamics for Scorpis with the CDR End-to-End Tune: II. Short-Pulse Stability

Carl Ekdahl

Abstract—An end-to-end simulation of Scorpis was performed for the Conceptual Design Report. This simulation used a tune significantly different than the tune used for assessing beam stability. Therefore, the stability assessment has been repeated with the end-to end tune in order to ensure that motion due to instabilities will not significantly blur the radiographic source spot.

I. INTRODUCTION

IN preparation for the conceptual design review of the Scorpis flash-radiography machine, a new tune of the magnetic transport through the linear induction accelerator (LIA) was developed for end-to-end (E2E) simulations [1]. Since this tune seems to be an efficient use of available magnetic field energy for beam transport and suppression of instabilities, we evaluated it for all of the beam physics concerns previously considered for the Conceptual Design Report (CDR) [2]. In this article I describe the evaluation of the three most dangerous instabilities that might affect single, short beam pulses.

The end-to-end simulations from cathode to target were performed by using Trak [3] to simulate the diode, then using the resulting distribution to launch the PIC slice code AMBER [4] through the LIA. Finally, AMBER, TRACE3D, or ENSOLVE were used to simulate beam transport through the downstream system to the radiation converter target [1]. Some of the results of this effort are summarized in Fig. 1.

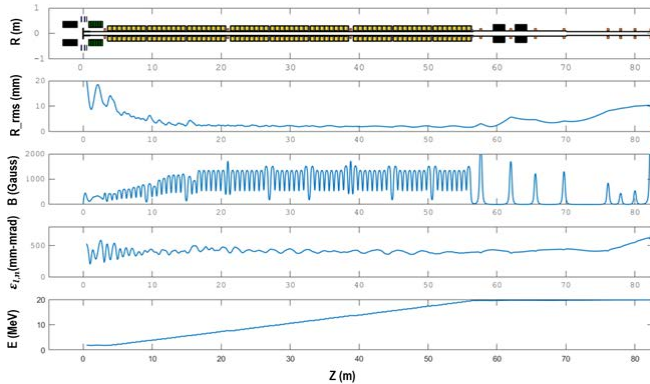


Fig. 1 : Results of end-to-end simulation of Scorpis. Top to bottom: Floor plan showing solenoids and accelerating gaps, beam rms radius, magnetic field on axis, normalized emittance, and beam energy.

Fig. 2 shows the matched beam transport through the E2E tune as calculated by the XTR envelope code [5]. Simulations of the matched beam envelope through this tune performed with the LAMDA envelope code and the LSP-Slice PIC code agreed with the envelope shown in this figure. Moreover, the PIC code results showed no evidence of emittance growth.

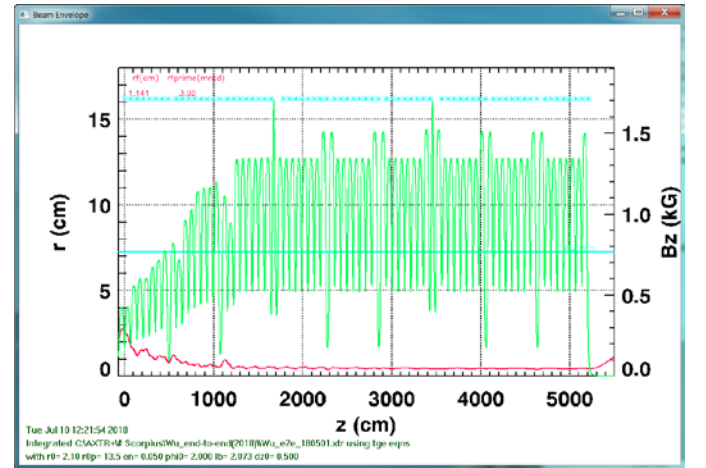


Fig. 2: Result of XTR envelope code simulation of Scorpis beam using the E2E magnetic tune. This simulation used the initial conditions listed in Table II. (Red) Beam envelope radius, (Green) Magnetic field on axis, (Cyan Line) Beam tube radius, (Cyan Asterisks) Relative cell voltages.

The radiographic source spot can be degraded by beam motion due to instabilities, even if they are not strong enough to disrupt the beam. We have previously assessed the following sources of motion for high-current LIAs, including Scorpis [6, 7, 8]:

- Beam Breakup (BBU) Instability
- Image Displacement Instability (IDI)
- Corkscrew Motion
- Ion Hose Instability
- Resistive Wall Instability
- Diocotron Instability
- Parametric Envelope Instability

The first two (BBU and IDI) are instabilities that can affect single pulses as short as a few tens of ns. Corkscrew motion can also blur spots from single short pulses. These concerns for single short pulses are the subject of this article. Although

also relevant for short pulses, the diocotron and envelope instabilities are of lesser concern for the conceptual design, and they will be considered in a future report.

II. UNSTABLE BEAM TRANSPORT

For this report I investigated the transported-beam stability for BBU, IDI and corkscrew, which are problematic for any short pulse in the Scorpius pulsetrain. As in previous stability calculations for the Scorpius CDR [7], I used the LAMDA beam dynamics code for this work. LAMDA models the beam as a string of n rigid disks (see Fig. 3). For a circular beam, the parameters associated with each disk are the current, energy, emittance, radius, and transverse centroid displacement. External Lorentz forces due magnetic fields, gaps, and walls are applied to each disk. It is assumed that there is no interaction between the beam disks, except at gaps (or due to wall resistivity, which is treated similarly). The resulting transverse motion is then calculated for each disk as it propagates, and output as a function of axial position. This provides the resulting beam motion at any given axial position as a function of time measured back from the beam head.

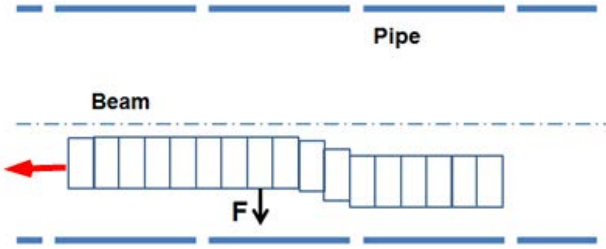


Fig. 3: In LAMDA, the beam pulse is represented by n disks. Forces due to external fields from magnets, gaps, wall images, etc. are applied to each disk.

A. Beam Breakup (BBU)

The most dangerous instability for electron linacs is the beam breakup (BBU) instability. For radiography LIAs it is particularly troublesome, because even if it is not strong enough to destroy the beam, the high-frequency BBU motion can blur the source spot, which is time-integrated over the over the pulse-length.

The BBU instability is the result of the beam deflection by transverse magnetic (TM_{1n0}) resonant modes of the accelerating cavities, which impresses an RF oscillation on the beam centroid position. In an LIA, the cavities are separated by lengths of beam pipe for which the cavity modes are cut off, so the cavities can only communicate with each other via beam centroid oscillations. Each successive cavity reinforces the beam oscillation, which eventually grows exponentially. Beam focusing reduces the oscillation amplitude, but if it is not strong enough, the amplification wins out. For a large enough number of accelerating cells, theory [9, 10, 11] predicts that the number of e-foldings asymptotes to

$$\Gamma = I_{kA} N_g Z_{\perp \Omega/m} \langle 1/B_{kG} \rangle / 3 \times 10^4 \quad (1)$$

where I_{kA} is the beam current in kA, N_g is the number of gaps, $Z_{\perp \Omega/m}$ is the transverse impedance in Ω/m , B_{kG} is the guide field in kG, and $\langle \rangle$ indicates averaging over z . This theoretical maximum amplitude of the BBU has been experimentally confirmed [12, 8], and it was used at DARHT to design magnetic field tunes that suppress BBU amplification to acceptable levels. Note that in these theories there is no stability threshold.

For this report, LAMDA simulations of BBU with the Scorpius E2E tune used a single frequency initial beam motion to excite the instability, which is analogous to experimental excitation with a tickler cavity. The frequency chosen for the simulation was the ~ 808 -MHz peak of the dominant mode. This is the worst case, because it produces the maximum growth. The growth of BBU calculated for Scorpius with the E2E tune is shown in Fig. 4 for a resonantly excited beam. For comparison, LAMDA calculation of resonantly excited BBU growth in DARHT-I is also shown. The tune for this DARHT-I simulation was the nominal tune used for many hydrotests [13]. As seen in this plot, the calculated BBU amplification at the exit of Scorpius is less than the calculated amplitude in DARHT, despite the longer length of the Scorpius LIA. The gain for resonant excitation at the frequency of maximum transverse impedance is 7.5 for the E2E tune on Scorpius, compared with a gain of 14 for DARHT-I. Moreover, the E2E tune provides a significant improvement over the CDR tune, which had a BBU gain of ~ 12 [7].

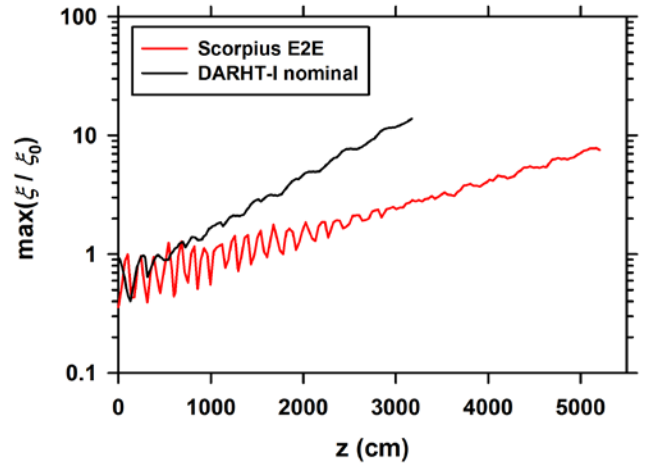


Fig. 4: BBU growth through the E2E tune compared with nominal tune for the DARHT-I LIA. These simulations were initially CW excited at 808 MHz, which is the peak of the transverse impedance resonance lineshape. Resonant excitation such as this produces the most virulent instability, and is the worst case that would ever be encountered in practice.

B. Image Displacement Instability (IDI)

The image displacement instability (IDI) is also the result of a slightly offset beam interacting with a cavity. However, while the BBU is the result of specific cavity resonance EM fields interacting with the beam, the IDI has no frequency dependence. It is the result of the difference of quasi-static

magnetic and electric field boundary conditions. Therefore, it can disrupt the beam even at the lowest frequencies. Moreover, unlike the BBU, the IDI does have a theoretical stability threshold. That is, the beam is stable in a guide field more than $B_{\min}(\gamma, I_b)$, which is a function of beam energy, current, and accelerator geometry. Thus, it is most dangerous at the entrance to the accelerator, where the magnetic field is low (Fig. 2). One particular theory [11] predicts stability for magnetic fields B such that

$$B_{kG}^2 / \gamma > 1.36 \left(\frac{w}{L} \right) \frac{I_{kA}}{b_{cm}^2} \quad (2)$$

where w is the gap width, b is the pipe radius, L is the cell spacing, and I is the beam current. Also, γ is the relativistic mass ratio. The quantity B^2 / γ , is plotted as a function of distance through the LIA in Fig. 5, which also shows the threshold given by Eq. (2). Although the numerical factor in this threshold can vary by factors of several between competing theories, it is evident that the IDI is prevented by the strength of the field in the E2E tune.

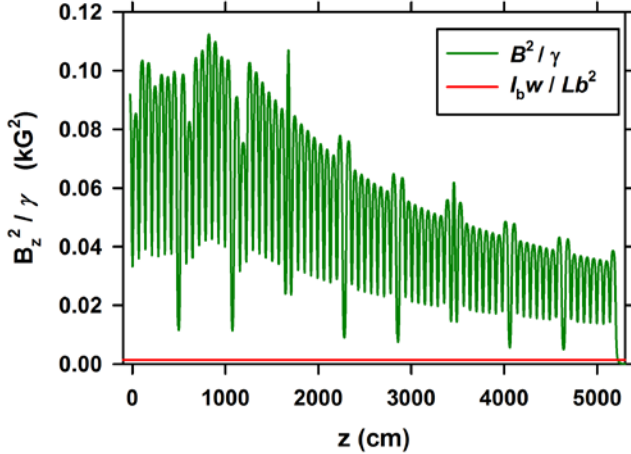


Fig. 5: Left side of Eq. (2) for the E2E tune, also showing the stability threshold for the Scorpis cell design in red.

C. Corkscrew Motion

Corkscrew motion is the result of temporal variation of the beam energy interacting with transverse magnetic fields in the LIA that are created by misalignment of the beam transport solenoids [14, 15, 16]. Corkscrew is a particular concern, because increasing the solenoidal magnetic field to suppress BBU also increases the misalignment fields, thereby also increasing corkscrew. Moreover, high-frequency corkscrew caused by the fast rising beam head can excite the BBU [17]. Although there are means for suppressing corkscrew using corrector dipoles embedded in the LIA cells [15, 18, 19, 20, 21], best engineering practices can do much to mitigate this cause of motion. Temporal variations of gap voltages that are the same on each cell add coherently through the LIA, and are

the worst case of corkscrew. This case is analyzed here for the E2E tune.

The amplitude of corkscrew motion is defined as

$$A^2 = \langle \delta x^2 \rangle_t + \langle \delta y^2 \rangle_t \quad (3)$$

where the brackets indicate averaging over time, and $\delta x = x - \langle x \rangle_t$, $\delta y = y - \langle y \rangle_t$ [15]. For coherent energy variations, a convenient scaling formula for the amplitude A after N misaligned solenoids is [16]

$$A \approx \sqrt{N} \delta \ell \phi \delta \gamma / \gamma \quad (4)$$

where $\delta \ell$ is the total rms misalignment (quadrature sum of horizontal, vertical, pitch, and yaw), γ is the relativistic mass factor, $\delta \gamma$ is its rms variation in time during the pulse, and ϕ is the total phase advance ($\phi = \int k_\beta dz$, where the betatron wavenumber is $k_\beta = eB_z / 2\beta\gamma m_e c = B_{kG} / 3.4\beta\gamma \text{ cm}^{-1}$). The factor $\phi \delta \gamma / \gamma = \delta \phi$ is the rms phase variation due to energy variations, and $\delta \ell B_z$ is proportional to the rms misalignment dipole strength. Eq. (4) represents the quadrature sum of deflections over all N cells. In Eq. (4) the number of cells is predetermined by the LIA design, and the total phase advance is ordained by other constraints on the tune (e.g., suppression of BBU). The remaining parameters subject to engineering control are $\delta \ell$ and $\delta \gamma$. These can be reduced by accurate alignment techniques, and by reduction of noise and fluctuations on the pulsed-power. Although Eq. (4) suggests that they can be simply traded one for the other, this bilinear scaling is only valid over a narrow range of parameters and small total phase advance [7]. Since with a low-energy injector the fractional coherent energy variation at the Scorpis exit is approximately proportional to the fractional gap-voltage variations, $\delta \gamma / \gamma \approx \delta V / V$, I use $\delta V / V$ as the variable parameter for corkscrew simulations.

In order to assess the maximum corkscrew motion that can be expected for Scorpis, I used LAMDA to simulate motion at the LIA exit for the maximum allowable misalignment offset and gap-voltage variation specified in the CDR ($\delta \ell < 0.2 \text{ mm}$, and $\delta V / V < 5\%$). An example of the random transverse magnetic fields calculated by LAMDA for the E2E tune with $\delta \ell < 0.20 \text{ mm}$ misalignment is shown in Fig. 6.

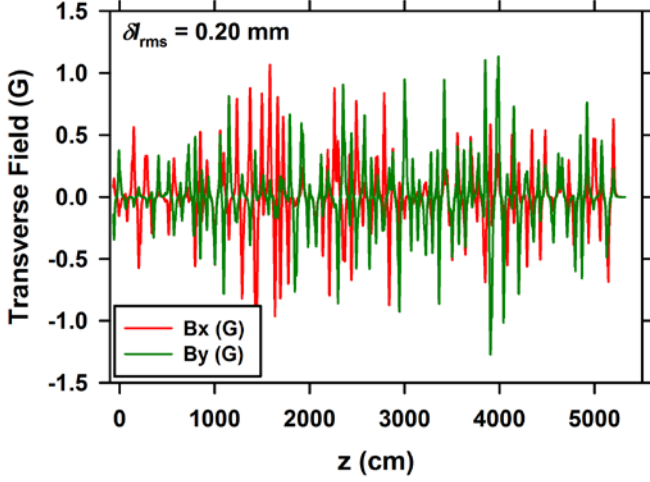


Fig. 6: A random distribution of transverse magnetic fields calculated by LAMDA for the E2E tune, and a total rms misalignment of 0.2 mm, which is the maximum specified in the CDR. The rms magnetic field for this distribution is 0.34 G.

Fig. 7 shows the current and voltage pulses that I used in LAMDA for simulations of corkscrew resulting from 5% rms voltage variations added coherently, which is the worst case. The range used for calculating the corkscrew amplitude (Eq. (3)) is also shown in this plot. This voltage waveform was applied to every accelerating gap to simulate coherent addition through the LIA.

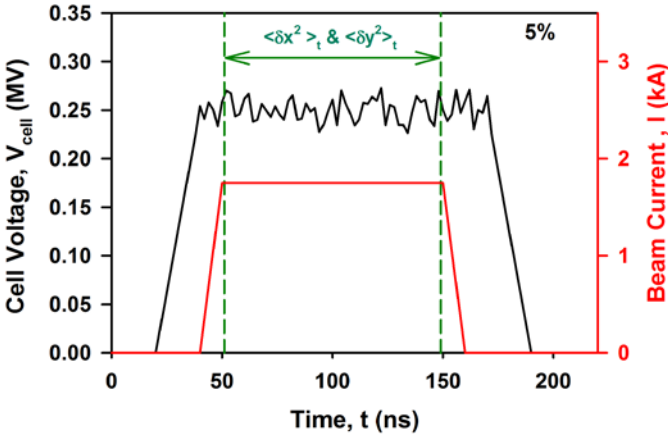


Fig. 7: Current (red) and voltage (black) wave forms used for LAMDA simulations with 5% rms voltage variation. Also shown in green is the range used for calculating the corkscrew amplitude A defined by Eq. (3).

The motion of the centroid at the LIA exit is shown in the next three illustrations. Fig. 8 and Fig. 9 are the time resolved horizontal and vertical positions of the beam centroid, showing the limits of motion due to cycloidal constraint of the beam by the axial magnetic field [20]. Fig. 10 shows the trajectory of the beam centroid due to the motion shown in Fig. 8 and Fig. 9.

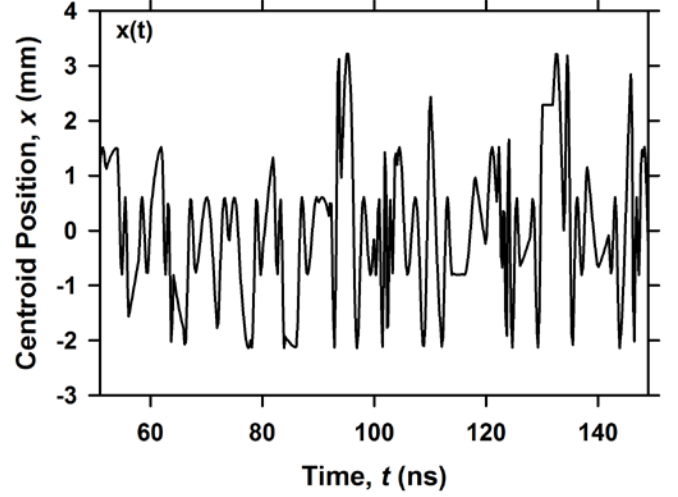


Fig. 8: LAMDA simulation of centroid horizontal position at the exit of the Scorpis LIA due to cell voltage fluctuations shown in Fig. 7 interacting with transverse magnetic fields shown in Fig. 6.

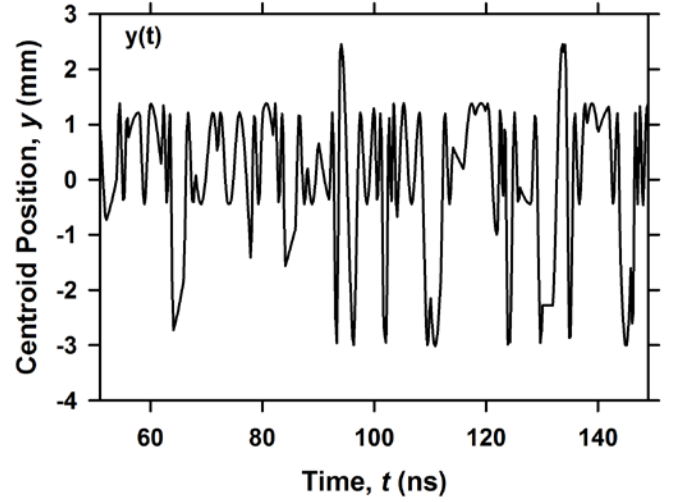


Fig. 9: LAMDA simulation of centroid vertical position at the exit of the Scorpis LIA due to cell voltage fluctuations shown in Fig. 7 interacting with transverse magnetic fields shown in Fig. 6.

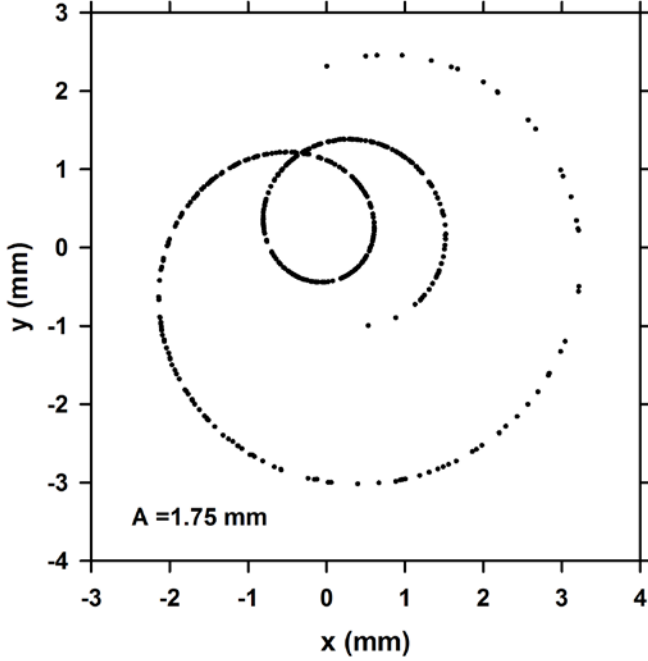


Fig. 10: LAMDA simulation of beam centroid position mapped out at LIA exit.

The LAMDA simulations yielded corkscrew amplitudes $A < 1.6$ mm for the E2E tune (averaged over several different randomizations of the offsets, but all with the same voltage waveform shown in Fig. 7). For comparison, the CDR tune, which was optimized to reduce corkscrew [7], produced $A < 1.5$ mm. Since the difference between these results is within the uncertainty of the calculations, there appears to be no advantage to using a tune designed to minimize corkscrew, contrary to analytic theory [7]. Moreover, these corkscrew amplitudes resulting from the maximum design tolerances for alignment and pulsed-power are easily corrected in practice by applying the tuning V algorithm [15, 18, 20, 21]. The engineering trade-off contour plot of misalignment vs voltage variation [7] is deferred until the preliminary LIA design is frozen, at which point another tune will be necessary, and the plot will be more relevant.

III. CONCLUSION

Beam-dynamics concerns were evaluated for the tune used in end-to-end simulations for the Scorpius CDR. In summary, the risks to radiographic performance due to these concerns can be readily mitigated through careful accelerator engineering and tuning as practiced at DARHT.

Simulations of matched-beam transport by the LSP-Slice PIC code showed no evidence of emittance growth, and agreed with the XTR and LAMDA envelope codes. LAMDA simulations of BBU had gain that was about half that of the nominal tune on DARHT-I. IDI was shown to be easily suppressed by the strength of the solenoidal focusing. LAMDA simulations of corkscrew due to the worst case expected for misalignment and pulsed power fluctuations had corkscrew amplitudes $A < 2$ mm. The simulated corkscrew

amplitudes for the E2E tune were about the same as those simulated for the CDR tune, which was designed to minimize this motion based on theory.

ACKNOWLEDGMENT

The author thanks his colleagues for lively discussions concerning beam stability and other accelerators topics. He also thanks the reviewers for carefully reading this report and suggesting improvements. This work was supported by the National Nuclear Security Administration of the U.S. Department of Energy under contract DE-AC52-06NA25396.

REFERENCES

- [1] Y. H. Wu and Y.-J. Chen, "End-to-end energy variation study for induction radiography accelerator," in *Int. Part. Accel. Conf.*, Copenhagen, DK, 2017.
- [2] C. Ekdahl, "Electron-beam dynamics for an advanced flash-radiography accelerator," *IEEE Trans. Plasma Sci.*, vol. 43, no. 12, pp. 4123 - 4129, Dec. 2015.
- [3] S. Humphries, "Technical information: TriComp Series," Field Precision, LLC, 2013. [Online]. Available: www.fieldp.com/technical.html.
- [4] J. L. Vay and W. Fawley, "AMBER user's manual," IAEA, 2000. [Online]. Available: http://www.iaea.org/inis/collection/NCLCollectionStore/_Public/32/069/32069294.pdf.
- [5] C. Ekdahl, "Beam Dynamics for Scorpius with the CDR end-to-end tune: I. Transport," Los Alamos National Laboratory Technical Report, LA-UR-18-, 2018.
- [6] C. Ekdahl, "Beam dynamics for ARIA," Los Alamos National Laboratory Report, LA-UR-14-27454, 2014.
- [7] C. Ekdahl, "Beam dynamics for the Scorpius Conceptual Design Report," Los Alamos National Laboratory Technical Report, LA-UR-17-29176, 2017.
- [8] C. Ekdahl, J. E. Coleman and B. T. McCuistian, "Beam Breakup in an advanced linear induction accelerator," *IEEE Tran. Plasma Sci.*, vol. 44, no. 7, pp. 1094 - 1102, 2016.
- [9] V. K. Neil, L. S. Hall and R. K. Cooper, "Further theoretical studies of the beam breakup instability," *Part. Acc.*, vol. 9, pp. 213-222, 1979.
- [10] G. Caporaso, "The control of beam dynamics in high energy induction linacs," in *Linear Accelerator Conf. (LINAC)*, 1986.
- [11] G. J. Caporaso and Y. -J. Chen, "Electron Induction Linacs," in *Induction Accelerators*, K. Takayama and R. J. Briggs, Eds., New York, Springer, 2011, pp. 117 - 163.
- [12] C. A. Ekdahl, E. O. Abayta, P. Aragon and et al., "Long-pulse beam stability experiments on the DARHT-II linear induction accelerator," *IEEE Trans. Plasma Sci.*, vol. 34, pp. 460-466, 2006.
- [13] D. C. Moir, *Personal communication*, 2012.

- [14] Y.-J. Chen, "Corkscrew modes in linear induction accelerators," *Nucl. Instrum. Methods Phys. Res.*, vol. A292, pp. 455 - 464, 1990.
- [15] Y.-J. Chen, "Control of transverse motion caused by chromatic aberration and misalignments in linear accelerators," *Nucl. Instr. Meth. in Phys. Res. A*, vol. 398, pp. 139 - 146, 1997.
- [16] Y.-J. Chen, "Transverse beam instability in a compact dielectric wall induction accelerator," in *Proc. 21st Particle Accel. Conf.*, Knoxville, TN, USA, 2005.
- [17] G. Caporaso, W. A. Barletta, D. L. Bix, R. J. Briggs, Y. P. Chong, A. G. Cole, T. J. Fessenden, R. E. Hester, E. J. Lauer, V. K. Neil, A. C. Paul, D. S. Prono and K. W. Struve, "Beam dynamics in the Advanced Test Accelerator (ATA)," in *5th Int. Conf. High Power Charged Particle Beams*, San Francisco, CA, USA, 1982.
- [18] J. T. Weir and a. et, "Improved ETA-II accelerator performance," in *Proc. 18th Particle Accel. Conf.*, New York, NY, USA, 1999.
- [19] K. C. D. Chan, C. A. Ekdahl, Y.-J. Chen and T. P. Hughes, "Simulation results of corkscrew motion in DARHT-II," in *Part. Accel. Conf.*, 2003.
- [20] C. Ekdahl and et al., "Suppressing beam motion in a long-pulse linear induction accelerator," *Phys. Rev. ST Accel. Beams*, vol. 14, p. 120401, 2011.
- [21] C. Ekdahl, "Tuning the DARHT long-pulse linear induction accelerator," *IEEE Trans. Plasma Sci.*, vol. 41, pp. 2774 - 2780, 2013.